RESEARCH ARTICLE

VOLCANICA

The abundance of submarine volcanism in arcs

Dallas H. Abbott*[α] and James L. Rubenstone[β,γ]

[α]Lamont-Doherty Earth Observatory of Columbia University, Palisades, NY 10964, USA.
[β]U.S. Nuclear Regulatory Commission, Washington, DC 20555, USA.
[γ]now at Link Technologies, Germantown, MD 20874, USA.

Abstract

Explosive submarine arc volcanoes can cause tsunamis, affect climate, and pose hazards to airplanes and ships. Although 70 % of the Earth is submarine, only 15 % of Holocene arc volcanoes in the Smithsonian Global Volcanism database are submarine. Merging locations of active submarine hydrothermal vents in arcs and the above database, we found 71 unlisted submarine arc volcanoes. Using Baker [2017, doi: 10.1016/j.oregeorev.2017.02.006], only 44 % of hydrothermal vents in arcs are known. Only 77 of the vent fields are on volcanoes in the Smithsonian database. Assuming that unknown submarine arc volcanoes are present in the same proportions as unknown vents, there are ~160 as-yet undiscovered Holocene age submarine arc volcanoes. Using geophysical data, we located 291 unsurveyed seamounts <30 km from arc axes, the distance within which active vents occur. We estimate 119±16 have active vents. Because more unknown seamounts exist, this means that >32 % of Holocene arc volcanoes are submarine.

Аннотация

Взрывные подводные дуговые вулканы могут вызывать цунами, воздействовать на климат и представлять опасность для воздушных и морских судов. Несмотря на то что 70 % поверхности Земли находится под водой, только 15 % вулканов голоценового периода в базе данных Smithsonian Global Volcanism являются подводными. Объединив данные об активных подводных гидротермальных источниках в дугах с вышеупомянутой базой данных, мы обнаружили 71 неучтенных подводных дуговых вулканов. Согласно Baker [2017, doi: 10.1016/j.oregeorev.2017.02.006], известно лишь о 44 % гидротермальных источников в находящихся в дугах. Только 77 из полей гидротермальных источников расположены на вулканах из базы данных Smithsonian. Предполагая, что неизвестные подводные дуговые вулканы присутствуют в том же соотношении, что и неизвестные источники, существует примерно 160 до сих пор неоткрытых подводных дуговых вулканов голоценового периода. Используя геофизические данные мы обнаружили 291 неисследованный подводный хребет в пределах <30 км от осей дуг, в пределах которых находятся активные источники. Мы оцениваем, что 119±16 из них имеют активные источники. Поскольку существует еще больше неизвестных подводных хребтов, это означает, что более 32 % вулканов голоценового периода являются подводными.

Keywords: Volcanism; Submarine; Arc; Ice core; Holocene; Hydrothermal.

1 Introduction

Large submarine eruptions can be a source of explosions that can affect airline and ship traffic, adversely affect coral reefs, produce phytoplankton blooms, or produce tsunamis [Bryan et al. 2004; Gisler et al. 2006; Santana-Casiano et al. 2013; Manga et al. 2018; Lyons et al. 2019; Borrero et al. 2022; Lynett et al. 2022; Fauria et al. 2023; Ishii et al. 2023]. If sufficiently large and sulfur-rich, the emissions from a submarine eruption can also impact the climate [Witter and Self 2006; Cole-Dai et al. 2013]. Because the 70 % of the Earth covered by oceans includes many plate boundaries and intraplate magmatic areas, submarine volcanoes should be relatively common. Note that we use volcano in this paper as a generic term to indicate a center of eruptive activity, consistent with the usage in the Smithsonian Global Volcano database. In this sense, a Holocene volcano may be recognized through its bathymetry, topography, or other geologic indicators. We focus in this paper on the submarine volcanoes that are most likely to produce large explosive eruptions: those in convergent-boundary volcanic arcs. Notably, only 15 % of the arc volcanoes listed in the Smithsonian Global Volcanism database are submarine—either completely submerged, with submerged caldera floors, or with submarine magma vents (Table 1). As we will show, this is a serious underestimate.

The Smithsonian database began in 1968 as a record of events, rather than features, so its initial focus was on eruptions rather than mapped volcanoes[†]. At present, there are 929 volcanoes identified as "arc volcanoes" by the Smithsonian Global Volcanism Program. The underrepresentation of submarine eruptions in the Smithsonian data is in part due to eruptive events in remote areas of the oceans being less likely to have been observed through historic time. The specific locations of submarine volcanism are further under-identified for three additional reasons. The first is that the ocean basins are incompletely mapped [Wessel and Smith 1998; Mayer et al. 2018; Wölfl et al. 2019]. The smallest submarine volcanoes (radius less than ~4.4 km) are invisible in satellite altimetry and can only be confirmed by swath mapping. Second, it is much more difficult to determine if a submarine volcano is

*✉ dallashabbott@gmail.com

[†]https://en.wikipedia.org/wiki/Center_for_Short-Lived_Phenomena

Submitted: 2024-01-31 | Accepted: 2024-05-21 | Published: 2024-07-22

Editor: J. Farquharson | Typesetter: J. Farquharson

Table 1: Distribution of subaerial and submarine arc volcanoes in the Smithsonian database (https://volcano.si.edu/volcanolist_holocene.cfm). Downloaded August 18, 2022.

Category	Number	Percent
Identified arc volcanoes (Smithsonian only)	929	100.0
Top below sea level	63	6.8
Top above sea level but with submarine Volcanism	27	2.9
Top above sea level but with submarine caldera	50	5.4
Total Smithsonian submarine arc volcanoes	140	15.1

volcanically active, by which we mean that its most recent detected activity was during the Holocene. Prior to the MODIS satellite era (first launched in 1999), it was difficult to find the precise locations of eruptions that produced pumice rafts and consequent ocean discoloration. Satellite observations are critical for determining the source volcanoes for pumice rafts which can drift hundreds to thousands of kilometers after an eruption. For example, some pumice rafts from the 1883 Krakatau eruption in the strait between Java and Sumatra drifted into the southwest Indian Ocean and were found in 1884 on beaches in Madagascar [Kent and Frick 1984].

The incomplete mapping and sampling of the seafloor means that a high percentage of all submarine hydrothermal vents in arcs are as yet undiscovered [Baker 2017]. High-temperature hydrothermal activity can be relatively ephemeral at a given location. Individual high temperature hydrothermal vents (black smokers) are active for a brief time, typically about five to ten years [Desbruyères 1998]. Fields of black smoker vents can be rejuvenated and are active for ~300 years [Kennish et al. 1997]. Lower temperature hydrothermal vents last longer but finding them requires more effort. Thus, many Holocene submarine volcanoes with documented Holocene eruptions have no known hydrothermal vents. An additional complication is that discovery of deep sea hydrothermal vents requires adequate measurements in the right location. Hydrothermal plumes are carried downstream by deep sea currents and can be missed if the observation is too far from the vent, in the wrong direction from the vent, or if adequate depth spacing of water column measurements is not available. The final reason for the under-identification is that the markers of such eruptions can be challenging to recognize in the geologic record. Volcanic ash layers from a submarine eruption that are deposited close to its source volcano may be eroded and redistributed by the resulting pyroclastic density currents [Seabrook et al. 2023]. Submarine eruptions can produce abundant, non-magmatic water vapor from vaporization of sea water by the hot eruption entering the ocean. As a result, the eruptive cloud is much higher for a given level of explosivity; this disperses ash over a broader region and results in relatively thinner distal ash layers [Yuen et al. 2022]. Volcanic ash layers less than ~2 cm thick [Kutterolf et al. 2021] are fully bioturbated into deep sea sediments and are invisible in core photos. Some thinner ash layers can be detected by measuring magnetic susceptibility at 1 cm intervals on boxed, weighed samples but this is labor-intensive and rarely done. If a submarine volcano has had only relatively small eruptions (VEI 5 or less), detecting activity prior to the satellite era requires more extensive core sampling and core analyses than are typically available. For all of these reasons—low coverage by cores and water column geochemistry and incomplete seafloor mapping—many Holocene age submarine volcanoes are likely currently unknown.

2 Data sources and methods: Volcanoes with active hydrothermal vents

We used data on volcanoes with active hydrothermal vents from two sources: the Ridge vent database [Beaulieu et al. 2013]* and the recently released MARHYS Database 1.0 - MARine HYdrothermal Solutions Database [Diehl and Bach 2020]†. Our main source on Holocene volcanoes is the Smithsonian database [Global Volcanism Program 2013]‡. To determine which volcanoes identified as hydrothermally active were also listed by the Smithsonian, we merged the Smithsonian database of arc volcano locations with the locations of the hydrothermal vents. The merged data shows 77 hydrothermal vent fields on 74 unique edifices listed by the Smithsonian Global Volcanism Program and a further 71 hydrothermal vents along an arc but not associated with an arc volcano in the Smithsonian database. We checked each of these occurrences by plotting the locations of the vents and the highest point on the volcano using the global gridded topography on Geomapapp [Ryan et al. 2009]§. With one exception (a vent defined using ^{3}He anomalies), all of the venting sites plot well above any local bathymetric plain. This made it relatively straightforward to determine if the vent was on an arc volcano listed by the Smithsonian Global Volcanism Program or on an unlisted volcano.

In all but a few cases, the volcanoes with active hydrothermal vents that are not listed by the Smithsonian are more than 16 km distant from any volcano in the Smithsonian database (Supplementary Material 1 Table S1). The few exceptions are locations where volcanoes are particularly closely spaced and volcanic edifices are relatively small, for example in the Tonga arc. In no case was an unlisted volcano with active hydrothermal venting less than 7 km distant from any of the volcanoes listed by the Smithsonian Global Volcanism Program. Overall, it appears that close to half of the arc volcanoes with active hydrothermal venting are not listed by the Smithsonian database.

* https://vents-data.interridge.org/; (downloaded in May, 2022)
† https://doi.org/10.1594/PANGAEA.935649
‡ https://volcano.si.edu/
§ http://www.Geomapapp.org

Seventy-four volcanoes listed by the Smithsonian Global Volcanism Program have active hydrothermal venting (Supplementary Material 1 Table S2). The hydrothermal vents on these volcanoes are mostly within 5 km of the topographic peak of the volcano. On some of the larger volcanoes, in particular those with large calderas, there are hydrothermal vents as much as 16 km away from the topographic peak. For example the ~17 km wide Yali-Kos caldera (Hellenic arc) has a hydrothermal vent 15 km away from its topographic peak. The 17 to 23 km wide Aira caldera in the northern part of Kagoshima Bay (Japan) also has a hydrothermal vent 15 km away from the topographic peak. Note that the topographically highest point of a caldera is typically along the remaining caldera wall, not at the center of the pre-caldera volcano. These hydrothermal vents are located no more than half the distance to the caldera center, that is <7.5 km for Yali-Kos, and <8.5–11.5 km for Aira. Thus, if we use the location of the caldera center rather than the topographic peak on the caldera rims, these hydrothermal vents are no more than 4.5 km further away from the volcanic center than the maximum distance (7 km) at smaller eruptive centers with no caldera.

3 Dated volcanic eruptions on volcanoes with active hydrothermal vents

Forty-four volcanoes listed in the Smithsonian database have both active hydrothermal vents and a most recent recorded eruption during the Holocene (Supplementary Material 1 Table S3). Although the life time of most high temperature hydrothermal vent fields is only about 300 years, the radiocarbon dates of the most recent volcanic eruptions on volcanoes with active hydrothermal vents are as old as 8040±90 B.C.E. This date is assigned to Palinuro in the Mediterranean based on a calibrated ^{14}C age [Global Volcanism Program 2013]. No more recent activity is identified for this volcano in the Smithsonian database. Given its location in the Mediterranean, the lack of identified later activity is unlikely to be the result of poor historical observations of the volcano. Overall, the distribution of dates is highly skewed towards younger ages (and higher temperature vents) (Figure 1). Of the volcanoes with active hydrothermal vents, 84 % had their most recent volcanic eruption during the last 145 years. Of these volcanoes, 27 % had their most recent volcanic eruption during the last 10 years. With one exception (Piip in the western Aleutians/Komandorsky arc), the submarine volcanoes with hydrothermal activity and with the oldest eruption ages (Table 2) are in areas with detailed studies of volcanic history [Clift and Blusztajn 1999; Wright and Gamble 1999; Horz 2002; Wright et al. 2006; Klaver et al. 2015; Kutterolf et al. 2021]. We therefore conclude that all of the volcanoes with identified active hydrothermal vents are of Holocene age and that most have probably had some eruptive activity within the last 200 years.

4 Results: The abundance of submarine volcanism in arcs

We estimate the abundance of unrecognized submarine volcanoes in arcs using two methods. The first follows Baker's [2017] linear regressions for the occurrence of hydrothermal vents along the length of an arc. The second method uses data on hydrothermal activity from a relatively well-studied arc (Tonga-Kermadec) to estimate the likelihood that bathymetric features near the arc axis at other arcs may be hydrothermally active.

4.1 Estimating abundance using inferred frequency of hydrothermal vents along arc length

Most of the known submarine volcanoes are located in intraoceanic arcs, that are built on thin crust (<30 km thick) and are composed mostly of small islands or submerged volcanoes. Some "island" arcs are built on thicker crust (>30 km), but are surrounded by ocean and have hydrothermal vents. From the data available at the time, Baker [2017] estimated that well-studied intraoceanic arcs have 1.8 hydrothermal vents per 100 km and island arcs built on thicker crust have 0.9 hydrothermal vents per 100 km. If one translates Baker's estimates into estimates of the abundance of hydrothermal vents in arcs (Table 3), there should be 261 hydrothermal vent fields on 261 volcanoes. All but three of the 148 known hydrothermal vent fields in arcs are on separate volcanic edifices. Using the number of unique volcanic edifices with hydrothermal vents (145), this translates into a deficit of 116 undiscovered hydrothermal vents on arc volcanoes (Table 3). Because this number does not take into account non-Smithsonian volcanoes that were not included in Baker's calculation, the actual number of undiscovered submarine volcanoes is likely more than 116.

Baker's estimates of hydrothermal vent abundance in the two types of island arcs is broadly consistent with what we know about volcanic volumes per unit time in arc volcanoes. As we will show, the best studied interoceanic arcs (Izu-Bonin-Marianas, Tonga-Kermadec) have more documented hydrothermal vent abundance than the best studied arcs on continental crust with islands (Aeolian, Hellenic/Aegean). However, oblique convergence also reduces volcano and consequent hydrothermal vent abundance, as is seen in the Komandorsky arc. Overall, in part due to logistical challenges in remote areas, there has not been enough study of the abundance of hydrothermal vents in most intraoceanic arcs and continental arcs with islands.

The global discovery rate of hydrothermal vents has been relatively constant at ~20 per year over the past few decades primarily by using techniques such as the presence of Mn- and Fe-rich plumes, oxidation-reduction anomalies, and particle rich discharge into the water column [Baker et al. 2016; Baker 2017]. All of the 148 hydrothermal vents in our combined database are on arc volcanoes. Most of the vents in the database represent the only venting sites on their volcanic edifice. A venting site can encompass multiple points with egress of hydrothermal fluids but the individual sites are extremely spatially restricted, usually less than 100 meters in diameter. In the MARHYS Database, the measurements from the same venting site often have the same latitude and longitude even when their locations are reported to six decimal places. Repeat measurements at the same site are at most a few kilometers apart [Baker et al. 2016].

Table 2: Six oldest dates of the most recent eruption of volcanoes with active hydrothermal vents and the methods used to estimate/measure ages and temperatures (Age/Temperature). Abbreviations. Ages: ^{14}Cc = calibrated carbon 14, ^{14}Cu = uncalibrated carbon 14. Tephra = tephrochronology, Obs = historical observations, Temperature Estimates: ROV = Remote Operated Vehicle, Sub = Crewed Submarine, Camera = deep towed camera, Scuba = Scuba divers.

Date last eruption	Hydrothermal site name	Volcanic Arc	Vent T (°C)	Age/Temperature
8040±90 BCE	Palinuro West	Aeolian Arc	54	^{14}Cc/ROV
5050±? BCE	Piip	Komandorsky	133	Tephra/Sub
4360±200 BCE	McCauley Caldera	Kermadec	?	^{14}Cu/Camera
350±100 BCE	Tutum Bay Ambitle I.	Tabar-Feni	98	^{14}Cu/Scuba
258±18 BCE	Methana	Hellenic	Low	Obs/Scuba
140±300 CE	Milos	Hellenic	123	^{14}Cu/ROV

Table 3: Calculating the number of undiscovered hydrothermal vents in arcs.

Arc type	Arc length (km)	No. of vents
Intraoceanic arcs	7000	126
Island arcs (continental crust)	15 000	135
Expected number vents		261
Observed number vents (multiples removed)		145
Vent deficit (based on Baker [2017])		116
Other		
Percentage known vents		56
Percentage unknown hydrothermal vents		44
Number unknown Holocene volcanoes (71/0.44)		160

Table 4: Submarine hydrothermal vents included in and absent from the Smithsonian database. Estimate of undiscovered Holocene age volcanoes with submarine hydrothermal vents. % volcanoes: Values with no parentheses are relative to the Smithsonian Database. Values in parentheses are corrected to include inferred unknown volcanoes.

Category	Number	% volcanoes	
Smithsonian arc volcanoes; all	929	100	(80)
Smithsonian submarine	140	15	(12)
Hydrothermal; not in Smithsonian	71	8	(6)
Hydrothermal; not yet found	160	17	(14)
Total submarine arc volcanoes	371	40	(32)

Table 5: Active hydrothermal vents: abundance versus distance from Tonga-Kermadec arc axis. Because the areas far from the axis of the arc are not well surveyed, the number of inactive seamounts from 15 to 30 km from the arc axis is estimated as the sum of the number of inactive seamounts less than 15 km from the axis. The number in parenthesis (7) is the number of inactive seamounts documented in the literature. The number of inactive seamounts from 30 to 60 km is also estimated as the sum of the number of inactive seamounts from 0 to 30 km from the axis. The uncertainty estimate assumes that the number of hydrothermally active seamounts could differ by ±2 seamounts in each distance group.

Distance to axis	Number active	Number inactive	% active	% uncertainty
0 to 3.5	33	5	87	5
3.5 to 15	11	23	32	6
15 to 30	10	28 (7)	26	5
30 to 60	0	56	0	0

Only three of the vents in our database are multiple venting sites identified on a single volcanic center. Two multiple sites are on the ~17 km wide Kos-Yali caldera in the Hellenic Arc. One multiple site is on the 9–12 km wide Monowai caldera in the Kermadec arc [Paulatto et al. 2014]. We assume that the undiscovered hydrothermal vents are distributed in the

Table 6: Active hydrothermal vents: abundance versus distance from Tonga-Kermadec arc axis. Because the areas far from the axis of the arc are not well surveyed, the number of inactive seamounts from 15 to 30 km from the arc axis is estimated as the sum of the number of inactive seamounts less than 15 km from the axis. The number in parenthesis (7) is the number of inactive seamounts documented in the literature. The number of inactive seamounts from 30 to 60 km is also estimated as the sum of the number of inactive seamounts from 0 to 30 km from the axis. The uncertainty estimate assumes that the number of hydrothermally active seamounts could differ by ±2 seamounts in each distance group.

Axial distance (km)	Seamounts (total number)	Active		
		Minimum number (%)	Mean number (%)	Maximum number (%)
0 to 3.5	57 (20%)	47 (16%)	50 (17%)	53 (18%)
3.5 to 15	126 (43%)	33 (11%)	41 (14%)	48 (17%)
15 to 30	108 (37%)	23 (8%)	28 (10%)	34 (12%)
30 to 60	0 (0%)	0 (0%)	0 (0%)	0 (0%)
Sum	291 (100%)	103 (35%)	119 (41%)	135 (46%)

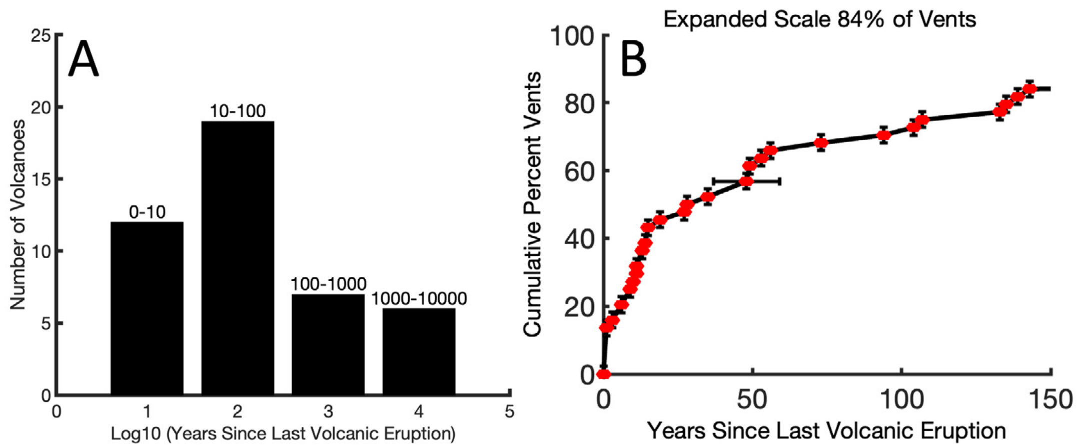

Figure 1: Distribution of dates of most recent volcanism on volcanoes with submarine hydrothermal activity. Data from [Global Volcanism Program 2013]. [A] All eruptions. Four of the six oldest eruptions were dated using the ^{14}C method, one was dated by tephrochronology and one through historical observations (Table 2). All of the younger eruptions were directly observed. [B] Cumulative frequency of volcanoes with hydrothermal vents with their most recent volcanic eruption within the last 150 years.

same proportion as in our database: between arc volcanoes in the Smithsonian Global Volcano database (Table 4) and arc volcanoes not in the Smithsonian Global Volcano database. Applying our estimate of undiscovered hydrothermal activity in arcs (44 % of all vents) to our finding of 71 unrecognized arc volcanoes indicates that ~160 Holocene age volcanoes with hydrothermal vents are as yet unrecognized as volcanically active (Figure 2, Table 3). This number of volcanoes assumes that each "undiscovered" hydrothermal vent corresponds to a unique volcano, although a few of the largest volcanoes may have multiple hydrothermal vents. As previously noted, the relatively short time that a hydrothermal vent may be active suggests additional undiscovered submarine volcanoes exist within intraoceanic arcs.

Volcanoes with submarine hydrothermal vents are found at over half of the intraoceanic arc volcanoes in the well-studied Tonga-Kermadec, Izu-Bonin, and Mariana arcs (Figure 3, Figure 4). Tonga-Kermadec is particularly well studied and is the only arc for which both hydrothermally active and inactive volcanoes are well documented (Figure 3, Supplementary Material 1 Table S5). Nevertheless, our data on poorly studied seamounts suggests that some hydrothermal vents may yet be discovered even in these best-studied intraoceanic arcs. Arcs that require much more exploration and mapping to identify all hydrothermally active submarine volcanoes are the intraoceanic portions of the Aleutian-Komandorsky arc, the Banda-Lesser Sunda Arc, the Fiji arc, the Halmahera Arc, the Kurile arc, Lesser Antilles arc, the Luzon arc, the New Britain arc, the Rykyuyu arc, the San Cristobal-Vanuatu arc, the Solomons Arc, the South Sandwich arc, the Sulawesi arc, and the Tabar-Feni arc (Figures 4, 5, 6 and 7). In all of these arcs there are large numbers of poorly studied submarine volcanoes that are potentially hydrothermally active. The relationship of hydrothermal activity to distance from the arc axis is discussed in the next section.

4.2 Quantifying hydrothermal vent abundance using distance from arc axis

The deficit in hydrothermal vents and their associated volcanoes can also be quantified by calculating the distance from the axis of the arc versus the number of volcanoes with active and inactive hydrothermal vents. We define the axis of the arc

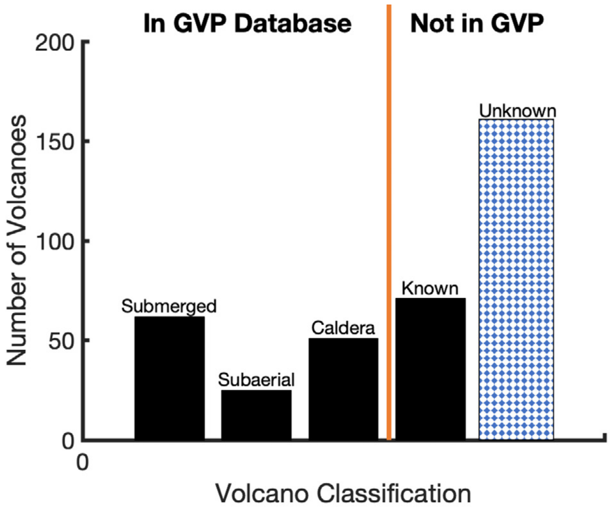

Figure 2: Distribution of submarine volcanic types. Submerged: no part of the volcano is subaerial. Subaerial: volcano has subaerial portions but also submarine lava vents. Caldera: volcano has subaerial portions but floor of caldera is below sea level. All of the preceding types of submarine volcanoes are listed by Global Volcanism Program [2013], are classified in Supplementary Material 1 Table S4 and are shown to the left of vertical red line. Existence of and depth of submarine caldera floor checked using Geomapapp. Right of vertical red line: Known: submarine volcano with active hydrothermal vents not listed by Global Volcanism Program [2013]. Unknown: (dotted bar) inferred number of as-yet unknown submarine volcanoes with active hydrothermal vents based on our data and Baker [2017]. The unknown volcanoes are not in the Global Volcanism Project (GVP) database maintained by the Smithsonian Institution.

by interpolating between the locations of volcanoes listed by the Smithsonian Global Volcanism Program at a half-km spacing. The Tonga-Kermadec arc is the only intraoceanic arc that is both well studied and for which both hydrothermally active and inactive volcanoes have been well-defined in the literature [de Ronde et al. 2001; Baker et al. 2003; Stoffers et al. 2003; Arculus 2004; Stoffers et al. 2006; Wright et al. 2006; de Ronde et al. 2007; Graham et al. 2008; Baker et al. 2010; 2019; Walker et al. 2022]. In other intraoceanic arcs, there is little information about which volcanoes have been surveyed and found to be hydrothermally inactive. For example, although the Izu-Bonin arc seems to be well surveyed, the global hydrothermal database only lists 2 out of 12 hydrothermal vents as inactive. Similarly, the Marianas arc has 1 inactive vent listed out of a total of 25 hydrothermal vents.

Merging the locations of volcanoes with known hydrothermally active and inactive venting in the Tonga-Kermadec arc with the interpolated arc axis / centerline of the arc (Figure 3), shows a clear relationship of hydrothermal activity decreasing with distance from the arc axis (Table 5). Of the volcanoes located within 3.5 km of the arc axis, 87 % are hydrothermally active. This decreases to 32 % for those 3.5 to 15 km from the arc axis, and to 26 % for those located from 15 to 30 km from the arc axis. More than 30 km from the arc axis, there are no hydrothermally active volcanoes.

This distribution can be used to estimate the number of as-yet undiscovered hydrothermally active volcanoes in each arc. We use six datasets, all of which were carefully checked to avoid duplicates among them: the Smithsonian Global Volcanism Database, the two Hydrothermal Databases [Beaulieu et al. 2013; Diehl and Bach 2020], the latest Global Seamount database [Gevorgian et al. 2023], seamounts picked using topography in `Geomapapp` (Supplementary Material 1 Table S6) [Ryan et al. 2009], and our Tonga- Kermadec database (Supplementary Material 1 Table S5). Some volcanoes were picked visually along the arc axis using the bathymetry in `Geomapapp` [Ryan et al. 2009]. We made a cross-section of each volcano and selected those that had a sharp peak at the top or a clear caldera not yet filled with sediment. This strategy eliminated volcanos whose tops had been flattened by the addition of a reef or sediment infill; such volcanoes are likely to be pre-Holocene in age. We then calculated the distance from the arc axis of the unique volcanoes in the combined database of visual seamount picks and the latest global seamount database. Duplicates were eliminated. Out of the 291 remaining volcanoes from the merged database containing the visual seamount picks and the most recent seamount database (Supplementary Material 1 Table S6), 57 (20 %) are located within 3.5 km of the arc axis, 126 (43 %) within 3.5 to 15 km and 108 (37 %) within 15 to 30 km (Table 6). All of these 291 volcanoes are (so far as we know) as yet unstudied for hydrothermal activity. Based on the relationship between distance from the arc axis and hydrothermal activity observed in Tonga-Kermadec, 119±16 of these volcanoes are likely to be hydrothermally active.

The estimated number of hydrothermally active arc volcanoes (119±16) is a minimum estimate for several reasons. The first is that we picked active volcanoes using `Geomapapp` bathymetry [Ryan et al. 2009] along the apparent arc axis before we realized that some volcanoes further from the arc axis might also be hydrothermally active. Volcanoes located 15 to 30 km from the arc axis are undersurveyed for hydrothermal activity. We find the same pattern in the data from the Tonga-Kermadec arc. Seamounts 15 to 30 km from the arc axis are less likely to have been surveyed for hydrothermal activity. The second reason is that the updated global seamount database is based primarily on satellite altimetry and gravity gradients. As a result, it can only resolve the larger seamounts (>4.4 km in radius). In the Tonga-Kermadec arc, seamounts that are classified as separate edifices from detailed surveys, are often classified as a single volcano in the global seamount database. We also find that there is much less overlap between the individually picked volcanoes and the global seamount database than expected. This is because so many of the active volcanoes found using `Geomapapp` (120 out of an original 186) have a basal diameter that makes them too small to resolve using satellite altimetry and gravity gradients. The third reason is that the seafloor is incompletely mapped. In some areas the existing bathymetry is too poor to adequately pick small seamounts using `Geomapapp`. Finally, we are implicitly assuming that all seamounts that were hydrothermally active during the Holocene are presently hydrothermally active. Although there are a few hydrothermally active seamounts for

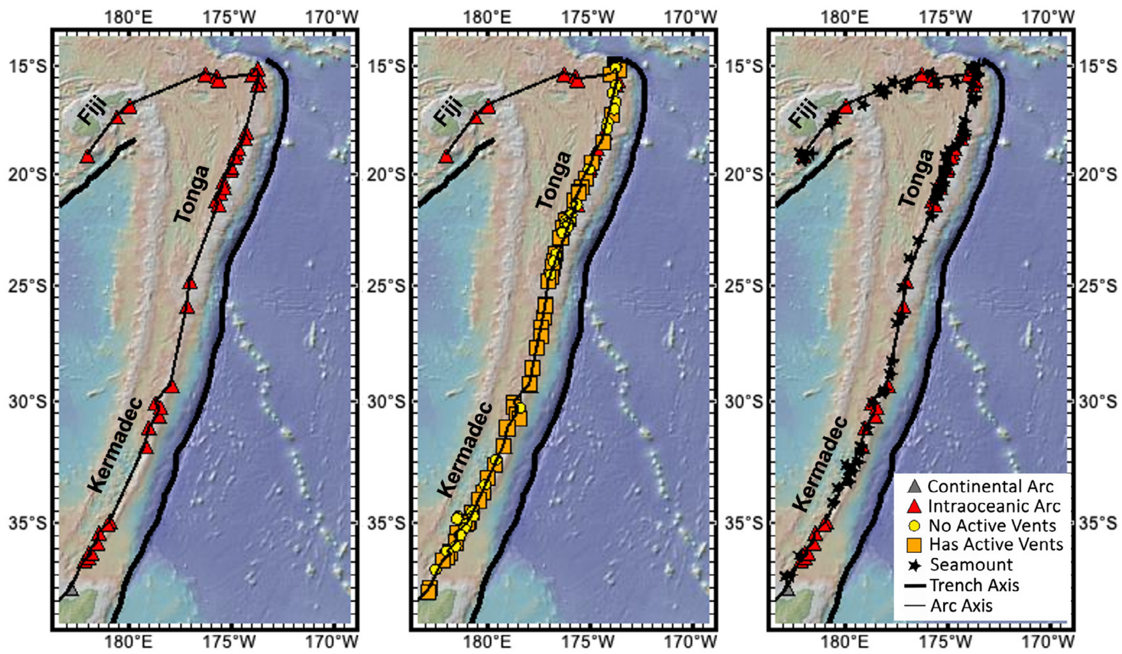

Figure 3: Map of arc volcanoes, hydrothermal vents and understudied seamounts in Fiji-Tonga-Kermadec arcs generated using Geomapapp [Ryan et al. 2009]. The data are separated into three separate panels so the locations of the arc volcanoes and the arc axis (left), hydrothermally active and inactive volcanoes (center) and seamounts as yet unstudied for hydrothermal activity (right) are clear. Red triangles: Intraoceanic arc volcanoes. Light black line: axis of the arc. Gray triangles: Continental arc volcanoes. Orange squares: Active submarine hydrothermal [Beaulieu et al. 2013; Diehl and Bach 2020]. Yellow circles: Volcanoes surveyed for hydrothermal activity but which are inactive. Heavy black lines: Location of trench axis. Black stars: Seamounts as yet unstudied for hydrothermal activity located within 30 km of arc axis.

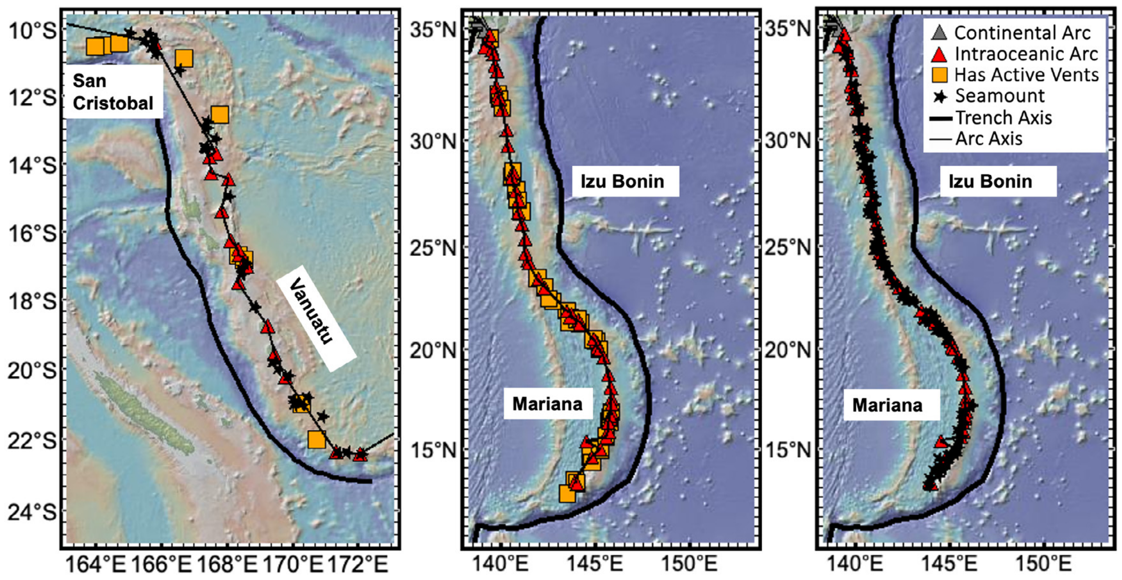

Figure 4: Map of arc volcanoes, hydrothermal vents and understudied seamounts in Izu-Bonin-Marianas (center and right panel) and San Cristobal-Vanuatu (left panel) arcs generated using Geomapapp [Ryan et al. 2009]. Red triangles: Intraoceanic arc volcanoes. Gray triangle: Continental arc volcanoes. Orange squares: Arc submarine hydrothermal vents [Beaulieu et al. 2013; Diehl and Bach 2020]. Heavy black lines: Location of trench axis. Black stars: Seamounts as yet unstudied for hydrothermal activity within 30 km of the arc axis. Light black line: axis of the arc.

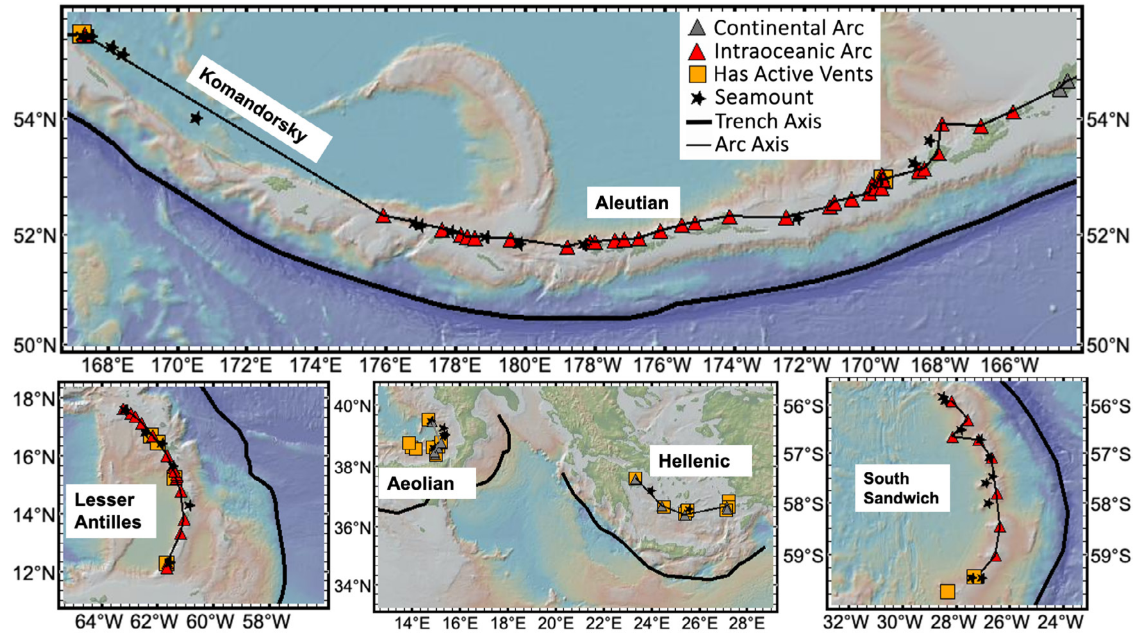

Figure 5: Map of arc volcanoes, hydrothermal vents and understudied seamounts in Aleutian-Komandorsky (top), Lesser Antilles (bottom left), Aeolian and Hellenic (bottom center) and South Sandwich (bottom right) arcs generated using Geomapapp [Ryan et al. 2009]. Red triangles: Intraoceanic arc volcanoes. Light black line: axis of the arc. Gray triangles: Continental arc volcanoes. The Aeolian and Hellenic arcs lie on continental crust but are partially submerged and contain hydrothermal vents. Their hydrothermal vents are largely well characterized but each contains a few unstudied seamounts. Orange squares: Active submarine hydrothermal vents [Beaulieu et al. 2013; Diehl and Bach 2020]. Heavy black lines: Location of trench axis. Black stars: Seamounts as yet unstudied for hydrothermal activity located within 30 km of arc axis.

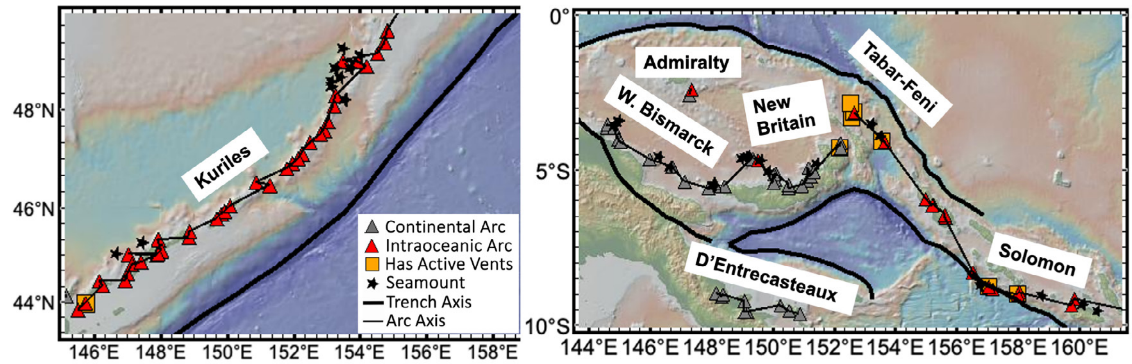

Figure 6: Map of arc volcanoes, hydrothermal vents and understudied seamounts in the Kuriles (left) and New Britain, Admiralty, Tabar-Feni and Solomon (right) arcs generated using Geomapapp [Ryan et al. 2009]. Red triangles: Intraoceanic arc volcanoes. Light black line: axis of the arc. Gray triangles: Continental arc volcanoes. Portions of the New Britain arc lie on continental crust but are partially submerged and contain hydrothermal vents. There are also submerged volcanoes on continental crust in the Western Bismarck Arc and in the D'Entrecasteaux Islands. Orange squares: Active submarine hydrothermal vents [Beaulieu et al. 2013; Diehl and Bach 2020]. Heavy black lines: Location of trench axis. Black stars: Seamounts as yet unstudied for hydrothermal activity located within 30 km of arc axis .

which the last volcanism was thousands of years ago (Table 2); 84 % of hydrothermally active seamounts last exhibited volcanism within the last 200 years. Submarine volcanoes that were volcanically active sometime during the Holocene do not necessarily exhibit active hydrothermal venting. Therefore, our original estimate of ~160 undiscovered Holocene seamounts is a minimum.

5 Discussion: Importance of identifying partially or fully submerged, Holocene volcanic edifices

Using ice cores drilled in Antarctica and Greenland, the largest sulfate loadings from volcanic eruptions are well documented and dated for the last 2500 years [Sigl et al. 2015]. These data are supplemented by historical records from Europe and Asia. Despite this, the source volcanoes for only seven of the twenty-

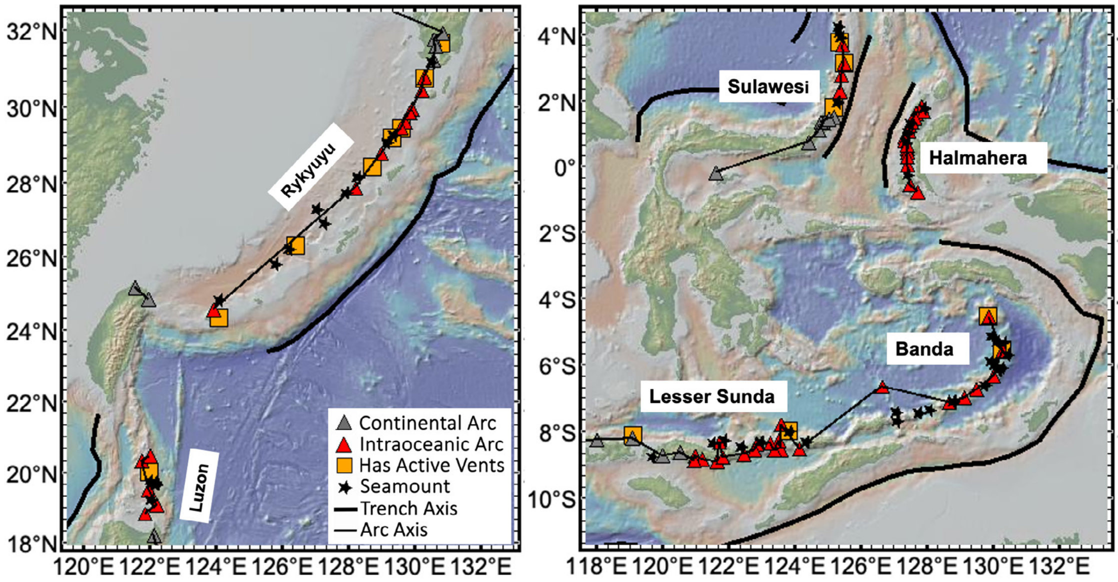

Figure 7: Map of arc volcanoes, hydrothermal vents and understudied seamounts in the Rykyuyu-Northern Luzon (left) and Lesser Sunda, Banda, Sulawesi and Halmahera (right) arcs generated using Geomapapp [Ryan et al. 2009]. Red triangles: Intraoceanic arc volcanoes. Light black line: axis of the arc. Gray triangles: Continental arc volcanoes. Portions of the Sulawesi and Lesser Sunda arc lie on continental crust but are partially submerged and contain hydrothermal vents. Orange squares: Active submarine hydrothermal vents [Beaulieu et al. 2013; Diehl and Bach 2020]. Heavy black lines: Location of trench axis. Black stars: Seamounts as yet unstudied for hydrothermal activity located within 30 km of arc axis.

three eruptions with the largest sulfate loadings have been identified. Five of these seven eruptions were from arc volcanoes, consistent with the high volatile and sulfur contents of most arc magmas. Only two of these volcanoes (Kuwae and Rabaul calderas) are on our list of submerged volcanoes. They represent 28 % of the identified sulfate source eruptions in arcs. If, as our analysis suggests, 32 % of all arc volcanoes are submarine and only 18 % are in the combined Smithsonian-hydrothermal vent database (Table 4), then 14 % of potential arc source volcanoes for the largest sulfate loading events are as yet unidentified as volcanoes active during Holocene time. If arc volcanoes represent the same proportion of the unidentified sources of sulfate loading (16) as do the seven identified sources, this means that there are at least two as-yet unidentified, submarine arc volcanoes whose eruptions produced severe sulfate loading during the last 2500 years. We say at least two because our estimates of unidentified submarine volcanoes are minima.

The 2022 eruption of Hunga Tonga-Hunga Ha'apai at 20.545 °S, 175,393 °W highlights the potential dangers of explosive eruptions from partially or fully submerged volcanic edifices. Despite a relatively low explosivity index of 6.3 [Purkis et al. 2023], the Hunga Tonga eruption produced large tsunami runup heights on nearby islands: 19 m in western Tongatapu, 20 m on south-eastern Nomuka Iki island and 20 m on southern Tofua [Borrero et al. 2022]. These islands are located between 65 to 90 km from the volcano. The runups are comparable to the near field tsunami runups from the 1883 Krakatau eruption [Symons et al. 1888; Self and Rampino 1981]. The Hunga Tonga eruption also caused tsunamis at much greater distances through an atmospheric pressure wave. The tsunami from Krakatau killed at least 36,000 people [Bryant 2014]. Largely because of the remoteness of the area, only four lives were lost to the Hunga Tonga tsunami [Borrero et al. 2022]. However, this would change with a submarine eruption with a higher VEI in a more populated region, in particular because the atmospheric tsunamis from Hunga Tonga arrived about 2 hours earlier than conventional tsunamis, lasted for over 5 days and produced tsunami wave heights of 2 meters at distances of 9000 km [Gusman et al. 2022; Lynett et al. 2022; Omira et al. 2022; Ramírez-Herrera et al. 2022]. The ash from the Hunga Tonga eruption also obscured sunlight in a large area of the ocean for a period of over ten days [Whiteside et al. 2023]. The reduction in light penetration to <10 meters may have had effects on biogeochemical processes in the ocean and on coral reefs [Santana-Casiano et al. 2013; Caron et al. 2019; Barone et al. 2022; Franz et al. 2024]. The eruption is also thought to have contributed to mid- and low-latitude ozone losses [Lu et al. 2023; Wang et al. 2023]. The pyroclastic density currents from the Hunga Tonga eruption eroded the seafloor, broke submarine communications cables up to 100 km from the volcano, and disrupted submarine life at least 100 km from the volcano [Seabrook et al. 2023]. Notably, the eruption did not have significant adverse effects on global climate. Although it was initially postulated that the immense amounts of water vapor produced by the Hunga Tonga eruption would warm the climate, the real climate effects were small and evident only at high latitudes [Bao et al. 2023].

The Hunga Tonga eruption represents a landmark study for several reasons. It showed that large volcanic eruptions in remote areas of the ocean can produce tsunamis on a global scale. There are 298 tsunamis in the global historical tsunami database maintained by NOAA whose source has never been identified [NGDC 2023]. The oldest tsunami with an unidentified source occurred in 2100 B.C.E. Some of these tsunamis with unknown sources could have been "Hunga Tonga-type" eruptions that were either never observed or never considered as a tsunami source because any potential volcanic initiator was was considered to be too far away from the location of the tsunami effects. Another lesson from the Hunga Tonga eruption is how far and how fast submarine pyroclastic density currents can travel; over 100 km away from the source volcano and at velocities of 122 km per hour [Clare et al. 2023; Seabrook et al. 2023]. This means that submarine cables can be broken very far away from a submarine eruption. It also means that passengers on ships within 100 km of an active submarine volcano could face grave danger. Appropriate safety protocols for ships and submarine cables located within 100 km of an awakened submarine volcano must be developed. Finally, the dilution of the sulfate signal from Hunga Tonga by vaporized seawater occurred due to the extensive heating of the surrounding ocean by eruptive products. One could imagine a different scenario, where the sulfate gases from a volcanic explosion reached the atmosphere before the caldera wall was breached by seawater. In that case, a large submarine eruption could produce significant climate cooling.

6 Conclusions and perspectives

Based on hydrothermal activity and existing bathymetric data, our analysis indicates that ~32 % of all arc volcanoes are submarine and many remain unidentified. The ~160 unidentified volcanoes which may have been active during the Holocene are most likely located in poorly studied portions of intraoceanic arcs. Using the statistics of active and inactive vent locations and their distance from the arc axis in the Tonga-Kermadec arc, a minimum of 119±16 undersurveyed seamounts globally are likely to be hydrothermally active. This is an underestimate because small volcanoes and volcanic centers 15 to 30 km from submarine arc axes are undercounted. By this, we mean that the volcanoes are too small to find using satellite altimetry and that there is as yet no multibeam bathymetry or conventional bathymetry that images their edifices.

Because arc hydrothermal vents are located on volcanic edifices and not on the sea floor, these arcs should be investigated in areas where swath mapping is not yet available and where most volcanic edifices are nearly completely or completely submerged. The water depth range of hydrothermal vents in the two vent databases ranges from 0 to 2960 meters [Beaulieu et al. 2013; Diehl and Bach 2020]. Techniques for finding the signature of hydrothermal venting by searching for anomalies in the water column (such as manganese sniffing or particle counters) should be applied within these depth ranges and within one km of swath-mapped volcanic edifices. Measurements of ^{3}He can find regions with active venting but are very difficult to use for precise location of hydrothermal vents.

Some authors found that volcanic volume per unit time is related most strongly to the proportion of arc perpendicular (i.e. trench normal) convergence [Sheldrake et al. 2020]. Others found that the probability of dangerous caldera eruptions is highest in arcs lacking back arc spreading centers and with high rates of trench normal convergence [Hughes and Mahood 2011]. Their map of the locations of giant caldera eruptions includes some intraoceanic arcs—notably the eastern Aleutians, the Izu-Bonin arc, the Rykyuyu, the Lesser Antllles, the Lesser Sunda arc, New Britain and Vanuatu. We suggest that mapping of hydrothermal vents and volcanic edifices in these arcs would yield the most benefit. An additional incentive to better map these particular arcs is the typical composition of the arc caldera magmas, which tend to be dacitic rather than rhyolitic. Although rhyolitic magmas can be highly explosive, they typically have lower sulfur contents than dacitic magmas. Notably, the two identified submarine arc volcanoes that produced significant sulfate loading (Kuwae and Rabaul) were both dacitic eruptions [Heming 1974; Witter and Self 2006].

Given this potentially large number of unidentified arc volcanic centers with unknown eruptive histories, it is not surprising then that volcanic sources have been identified for only seven of the 23 largest sources of sulfate loading observed in ice cores. Resolution of the remaining ice core signatures may benefit from further detailed investigations of underexplored intraoceanic arcs, in particular those with giant calderas that erupted dacitic magma: Vanuatu, Northern Rykyuyu, the Kuriles, Lesser Sundas, and the Lesser Antilles arcs. Analyses of new sediment cores near these arcs would also help to pinpoint the locations and ages of regionally extensive dacitic volcanic ashes.

Author Contributions

Abbott conceived the idea, wrote the initial draft of the paper, programmed the data merges and figures, and worked with `Geomapapp` to map volcanic edifices and to determine which volcanoes had submarine caldera floors. Rubenstone contributed insight on arcs and volcanic processes.

Acknowledgements

We thank Columbia University for access to the scientific literature and `MatLab` for the first author. The second author's contributions were done on his own time and do not represent a position of the U.S. Nuclear Regulatory Commission, the U.S. government or Link Technologies. We thank Malik Atadzhanov for the Russian translation of our abstract. We thank the editor Jamie Farquharson, reviewer Neil Mitchell and two unknown reviewers for insightful comments on earlier versions.

Data Availability

The data sources cited in this paper are all freely available on the web. Our data sources on volcanoes with active hydrothermal vents are the following: the Ridge vent database [Beaulieu et al. 2013] (https://vents-data.interridge.org/) (downloaded in May, 2022) and the recently released MARHYS Database 1.0 - MARine HYdrothermal Solutions Database [Diehl and Bach 2020] (https://doi.pangaea.de/10.1594/PANGAEA.935649). Our main source of data on Holocene volcanoes is the Smithsonian database (https://volcano.si.edu/) [Global Volcanism Program 2013]. Geomapapp is publicly available and is updated often with the latest bathymetry from detailed bathymetric surveys [Ryan et al. 2009].

Copyright notice

References

Arculus, R. A. (2004). *NoToVE-2004 (Northern Tonga Vents Expedition) Submarine hydrothermal plume activity and petrology of the northern Tofua Arc, Tonga*. Technical report. Voyage Summary SS11/2004.

Baker, E. T. (2017). "Exploring the ocean for hydrothermal venting: New techniques, new discoveries, new insights". *Ore Geology Reviews* 86, pages 55–69. DOI: 10.1016/j.oregeorev.2017.02.006.

Baker, E. T., R. A. Feely, C. E. J. De Ronde, G. J. Massoth, and I. C. Wright (2003). "Submarine hydrothermal venting on the southern Kermadec volcanic arc front (offshore New Zealand): location and extent of particle plume signatures". *Geological Society, London, Special Publications* 219(1), pages 141–161. DOI: 10.1144/gsl.sp.2003.219.01.07.

Baker, E. T., J. A. Resing, R. M. Haymon, V. Tunnicliffe, J. W. Lavelle, F. Martinez, V. Ferrini, S. L. Walker, and K. Nakamura (2016). "How many vent fields? New estimates of vent field populations on ocean ridges from precise mapping of hydrothermal discharge locations". *Earth and Planetary Science Letters* 449, pages 186–196. DOI: 10.1016/j.epsl.2016.05.031.

Baker, E. T., J. A. Resing, J. E. Lupton, S. L. Walker, R. W. Embley, K. H. Rubin, N. Buck, C. E. de Ronde, and R. J. Arculus (2010). "Multiple Active Volcanoes in the Northeast Lau Basin". *AGU Fall Meeting Abstracts*. Volume 2010, T13B-2188, T13B–2188.

Baker, E. T., S. L. Walker, G. J. Massoth, and J. A. Resing (2019). "The NE Lau Basin: Widespread and Abundant Hydrothermal Venting in the Back-Arc Region Behind a Superfast Subduction Zone". *Frontiers in Marine Science* 6. DOI: 10.3389/fmars.2019.00382.

Bao, Y., Y. Song, Q. Shu, Y. He, and F. Qiao (2023). "Tonga volcanic eruption triggered anomalous Arctic warming in early 2022". *Ocean Modelling* 186, page 102258. DOI: 10.1016/j.ocemod.2023.102258.

Barone, B., R. M. Letelier, K. H. Rubin, and D. M. Karl (2022). "Satellite Detection of a Massive Phytoplankton Bloom Following the 2022 Submarine Eruption of the Hunga Tonga-Hunga Haapai Volcano". *Geophysical Research Letters* 49(17). DOI: 10.1029/2022gl099293.

Beaulieu, S. E., E. T. Baker, C. R. German, and A. Maffei (2013). "An authoritative global database for active submarine hydrothermal vent fields". *Geochemistry, Geophysics, Geosystems* 14(11), pages 4892–4905. DOI: 10.1002/2013gc004998.

Borrero, J. C., S. J. Cronin, F. H. Latu'ila, P. Tukuafu, N. Heni, A. M. Tupou, T. Kula, O. Fa'anunu, C. Bosserelle, E. Lane, P. Lynett, and L. Kong (2022). "Tsunami Runup and Inundation in Tonga from the January 2022 Eruption of Hunga Volcano". *Pure and Applied Geophysics* 180(1), pages 1–22. DOI: 10.1007/s00024-022-03215-5.

Bryan, S., A. Cook, J. Evans, P. Colls, M. Wells, M. Lawrence, J. Jell, A. Greig, and R. Leslie (2004). "Pumice rafting and faunal dispersion during 2001–2002 in the Southwest Pacific: record of a dacitic submarine explosive eruption from Tonga". *Earth and Planetary Science Letters* 227(1–2), pages 135–154. DOI: 10.1016/j.epsl.2004.08.009.

Bryant, E. (2014). *The underrated hazard*. 3rd edition. Springer Berlin, Heidelberg. ISBN: 978-3-319-06133-7. DOI: https://doi.org/10.1007/978-3-319-06133-7.

Caron, V., J. Bailleul, F. Chanier, and G. Mahieux (2019). "Demise and recovery of Antillean shallow marine carbonate factories adjacent to active submarine volcanoes (Lutetian-Bartonian limestones, St. Bartholomew, French West Indies)". *Sedimentary Geology* 387, pages 104–125. DOI: 10.1016/j.sedgeo.2019.04.011.

Clare, M. A., I. A. Yeo, S. Watson, R. Wysoczanski, S. Seabrook, K. Mackay, J. E. Hunt, E. Lane, P. J. Talling, E. Pope, S. Cronin, M. Ribó, T. Kula, D. Tappin, S. Henrys, C. de Ronde, M. Urlaub, S. Kutterolf, S. Fonua, S. Panuve, D. Veverka, R. Rapp, V. Kamalov, and M. Williams (2023). "Fast and destructive density currents created by ocean-entering volcanic eruptions". *Science* 381(6662), pages 1085–1092. DOI: 10.1126/science.adi3038.

Clift, P. and J. Blusztajn (1999). "The trace-element characteristics of Aegean and Aeolian volcanic arc marine tephra". *Journal of Volcanology and Geothermal Research* 92(3–4), pages 321–347. DOI: 10.1016/s0377-0273(99)00059-1.

Cole-Dai, J., D. G. Ferris, A. L. Lanciki, J. Savarino, M. H. Thiemens, and J. R. McConnell (2013). "Two likely stratospheric volcanic eruptions in the 1450s C.E. found in a bipolar, subannually dated 800 year ice core record". *Journal of Geophysical Research: Atmospheres* 118(14), pages 7459–7466. DOI: 10.1002/jgrd.50587.

De Ronde, C. E. J., E. T. Baker, G. J. Massoth, J. E. Lupton, I. C. Wright, R. J. Sparks, S. C. Bannister, M. E. Reyners, S. L. Walker, R. R. Greene, J. Ishibashi, K. Faure, J. A. Resing, and G. T. Lebon (2007). "Submarine hydrothermal activity along the mid-Kermadec Arc, New Zealand: Large-scale effects on venting". *Geochemistry, Geophysics, Geosystems* 8(7). DOI: 10.1029/2006gc001495.

De Ronde, C. E. J., E. T. Baker, G. J. Massoth, J. E. Lupton, I. C. Wright, R. A. Feely, and R. R. Greene (2001). "Intra-oceanic subduction-related hydrothermal venting, Kermadec volcanic arc, New Zealand". *Earth and Planetary Science Letters* 193(3–4), pages 359–369. DOI: 10.1016/s0012-821x(01)00534-9.

Desbruyères, D. (1998). "Temporal variations in the vent communities on the East Pacific Rise and Galapagos Spreading Centre: a review of present knowledge". *Cahiers de Biologie Marine* 39(3-4), pages 241–244.

Diehl, A. and W. Bach (2020). "MARHYS (MARine HYdrothermal Solutions) Database: A Global Compilation of Marine Hydrothermal Vent Fluid, End Member, and Seawater Compositions". *Geochemistry, Geophysics, Geosystems* 21(12). DOI: 10.1029/2020gc009385.

Fauria, K. E., M. Jutzeler, T. Mittal, A. K. Gupta, L. J. Kelly, J. Rausch, R. Bennartz, B. Delbridge, and L. Retailleau (2023). "Simultaneous creation of a large vapor plume and pumice raft by the 2021 Fukutoku-Oka-no-Ba shallow submarine eruption". *Earth and Planetary Science Letters* 609, page 118076. DOI: 10.1016/j.epsl.2023.118076.

Franz, B. A., I. Cetinić, A. Ibrahim, and A. M. Sayer (2024). "Anomalous trends in global ocean carbon concentrations following the 2022 eruptions of Hunga Tonga-Hunga Ha'apai". *Communications Earth & Environment* 5(1). DOI: 10.1038/s43247-024-01421-8.

Gevorgian, J., D. T. Sandwell, Y. Yu, S.-S. Kim, and P. Wessel (2023). "Global Distribution and Morphology of Small Seamounts". *Earth and Space Science* 10(4). DOI: 10.1029/2022ea002331.

Gisler, G., R. Weaver, C. Mader, and M. Gittings (2006). "Two-dimensional simulations of explosive eruptions of Kick-Em Jenny and other submarine volcanos". *Caribbean Tsunami Hazard*. World Scientific. DOI: 10.1142/9789812774613_0006.

Global Volcanism Program (2013). *Volcanoes of the World, v. 4.3.4*. Edited by E. Venzke. Global Volcanism Program. DOI: 10.5479/si.gvp.votw4-2013.

Graham, I. J., A. G. Reyes, I. C. Wright, K. M. Peckett, I. E. M. Smith, and R. J. Arculus (2008). "Structure and petrology of newly discovered volcanic centers in the northern Kermadec–southern Tofua arc, South Pacific Ocean". *Journal of Geophysical Research: Solid Earth* 113(B8). DOI: 10.1029/2007jb005453.

Gusman, A. R., J. Roger, C. Noble, X. Wang, W. Power, and D. Burbidge (2022). "The 2022 Hunga Tonga-Hunga Ha'apai Volcano Air-Wave Generated Tsunami". *Pure and Applied Geophysics* 179(10), pages 3511–3525. DOI: 10.1007/s00024-022-03154-1.

Heming, R. F. (1974). "Geology and Petrology of Rabaul Caldera, Papua New Guinea". *Geological Society of America Bulletin* 85(8), page 1253. DOI: 10.1130/0016-7606(1974)85<1253:gaporc>2.0.co;2.

Horz, K. (2002). "Late Quarternary volcanic activity in the New Ireland Basin: Distribution and geochemical evolution of tephra at the Tabar-Lihir-Tanga-Feni chain, Papua New Guinea". PhD thesis. Christian-Albrechts Universität Kiel.

Hughes, G. R. and G. A. Mahood (2011). "Silicic calderas in arc settings: Characteristics, distribution, and tectonic controls". *Geological Society of America Bulletin* 123(7–8), pages 1577–1595. DOI: 10.1130/b30232.1.

Ishii, K., M. Hayashi, H. Ishimoto, and T. Shimbori (2023). "Prediction of volcanic ash concentrations in ash clouds from explosive eruptions based on an atmospheric transport model and the Japanese meteorological satellite Himawari-8: a case study for the Kirishima-Shinmoedake eruption on April 4th 2018". *Earth, Planets and Space* 75(1). DOI: 10.1186/s40623-023-01790-y.

Kennish, M. J., R. A. Lutz, and A. S. Pooley (1997). "'Residence Time' of Vesicomyid Clam Shells in Deep-sea Hydrothermal Vent Fields". *RIDGE Events* 8 (2), pages 6–9.

Kent, L. E. and C. Frick (1984). "Drift pumice in the Indian and South Atlantic Oceans". *South African Journal of Geology* 87(1), pages 19–33. DOI: 10.10520/EJC-1158c3dad3.

Klaver, M., T. Djuly, S. de Graaf, A. Sakes, J. Wijbrans, G. Davies, and P. Vroon (2015). "Temporal and spatial variations in provenance of Eastern Mediterranean Sea sediments: Implications for Aegean and Aeolian arc volcanism". *Geochimica et Cosmochimica Acta* 153, pages 149–168. DOI: 10.1016/j.gca.2015.01.007.

Kutterolf, S., A. Freundt, T. H. Druitt, J. McPhie, P. Nomikou, K. Pank, J. C. Schindlbeck-Belo, T. H. Hansteen, and S. R. Allen (2021). "The Medial Offshore Record of Explosive Volcanism Along the Central to Eastern Aegean Volcanic Arc: 2. Tephra Ages and Volumes, Eruption Magnitudes and Marine Sedimentation Rate Variations". *Geochemistry, Geophysics, Geosystems* 22(12). DOI: 10.1029/2021gc010011.

Lu, J., S. Lou, X. Huang, L. Xue, K. Ding, T. Liu, Y. Ma, W. Wang, and A. Ding (2023). "Stratospheric Aerosol and Ozone Responses to the Hunga Tonga-Hunga Ha'apai Volcanic Eruption". *Geophysical Research Letters* 50(4). DOI: 10.1029/2022gl102315.

Lynett, P., M. McCann, Z. Zhou, W. Renteria, J. Borrero, D. Greer, O. Fa'anunu, C. Bosserelle, B. Jaffe, S. La Selle, A. Ritchie, A. Snyder, B. Nasr, J. Bott, N. Graehl, C. Synolakis, B. Ebrahimi, and G. E. Cinar (2022). "Diverse tsunamigenesis triggered by the Hunga Tonga-Hunga Ha'apai eruption". *Nature* 609(7928), pages 728–733. DOI: 10.1038/s41586-022-05170-6.

Lyons, J. J., M. M. Haney, D. Fee, A. G. Wech, and C. F. Waythomas (2019). "Infrasound from giant bubbles during explosive submarine eruptions". *Nature Geoscience* 12(11), pages 952–958. DOI: 10.1038/s41561-019-0461-0.

Manga, M., K. E. Fauria, C. Lin, S. J. Mitchell, M. P. Jones, C. E. Conway, W. Degruyter, B. Hosseini, R. Carey, R. Cahalan, B. F. Houghton, J. D. White, M. Jutzeler, S. A. Soule, and K. Tani (2018). "The pumice raft-forming 2012 Havre submarine eruption was effusive". *Earth and Planetary Science Letters* 489, pages 49–58. DOI: 10.1016/j.epsl.2018.02.025.

Mayer, L., M. Jakobsson, G. Allen, B. Dorschel, R. Falconer, V. Ferrini, G. Lamarche, H. Snaith, and P. Weatherall (2018). "The Nippon Foundation—GEBCO Seabed 2030 Project: The Quest to See the World's Oceans Completely Mapped by 2030". *Geosciences* 8(2), page 63. DOI: 10.3390/geosciences8020063.

National Geophysical Data Center (NGDC) (2023). "Global Historical Tsunami Database". *NOAA National Centers for Environmental Information*. DOI: 10.7289/V5PN93H7. [Dataset].

Omira, R., R. S. Ramalho, J. Kim, P. J. González, U. Kadri, J. M. Miranda, F. Carrilho, and M. A. Baptista (2022). "Global Tonga tsunami explained by a fast-moving atmospheric source". *Nature* 609(7928), pages 734–740. DOI: 10.1038/s41586-022-04926-4.

Paulatto, M., A. B. Watts, and C. Peirce (2014). "Potential field and bathymetric investigation of the Monowai volcanic centre, Kermadec Arc: implications for caldera formation and volcanic evolution". *Geophysical Journal International* 197(3), pages 1484–1499. DOI: 10.1093/gji/ggt512.

Purkis, S. J., S. N. Ward, N. M. Fitzpatrick, J. B. Garvin, D. Slayback, S. J. Cronin, M. Palaseanu-Lovejoy, and A. Dempsey (2023). "The 2022 Hunga-Tonga megatsunami: Near-field simulation of a once-in-a-century event". *Science Advances* 9(15). DOI: 10.1126/sciadv.adf5493.

Ramírez-Herrera, M. T., O. Coca, and V. Vargas-Espinosa (2022). "Tsunami Effects on the Coast of Mexico by the Hunga Tonga-Hunga Ha'apai Volcano Eruption, Tonga". *Pure and Applied Geophysics* 179(4), pages 1117–1137. DOI: 10.1007/s00024-022-03017-9.

Ryan, W. B. F., S. M. Carbotte, J. O. Coplan, S. O'Hara, A. Melkonian, R. Arko, R. A. Weissel, V. Ferrini, A. Goodwillie, F. Nitsche, J. Bonczkowski, and R. Zemsky (2009). "Global Multi-Resolution Topography synthesis". *Geochemistry, Geophysics, Geosystems* 10(3). DOI: 10.1029/2008gc002332.

Santana-Casiano, J. M., M. González-Dávila, E. Fraile-Nuez, D. de Armas, A. G. González, J. F. Domínguez-Yanes, and J. Escánez (2013). "The natural ocean acidification and fertilization event caused by the submarine eruption of El Hierro". *Scientific Reports* 3(1). DOI: 10.1038/srep01140.

Seabrook, S., K. Mackay, S. J. Watson, M. A. Clare, J. E. Hunt, I. A. Yeo, E. M. Lane, M. R. Clark, R. Wysoczanski, A. A. Rowden, T. Kula, L. J. Hoffmann, E. Armstrong, and M. J. M. Williams (2023). "Volcaniclastic density currents explain widespread and diverse seafloor impacts of the 2022 Hunga Volcano eruption". *Nature Communications* 14(1). DOI: 10.1038/s41467-023-43607-2.

Self, S. and M. R. Rampino (1981). "The 1883 eruption of Krakatau". *Nature* 294(5843), pages 699–704. DOI: 10.1038/294699a0.

Sheldrake, T., L. Caricchi, and M. Scutari (2020). "Tectonic Controls on Global Variations of Large-Magnitude Explosive Eruptions in Volcanic Arcs". *Frontiers in Earth Science* 8. DOI: 10.3389/feart.2020.00127.

Sigl, M., M. Winstrup, J. R. McConnell, K. C. Welten, G. Plunkett, F. Ludlow, U. Büntgen, M. Caffee, N. Chellman, D. Dahl-Jensen, H. Fischer, S. Kipfstuhl, C. Kostick, O. J. Maselli, F. Mekhaldi, R. Mulvaney, R. Muscheler, D. R. Pasteris, J. R. Pilcher, M. Salzer, S. Schüpbach, J. P. Steffensen, B. M. Vinther, and T. E. Woodruff (2015). "Timing and climate forcing of volcanic eruptions for the past 2,500 years". *Nature* 523(7562), pages 543–549. DOI: 10.1038/nature14565.

Stoffers, P., T. Worthington, and S. S. Party (2003). *Cruise Report SONNE 167, Louisville Ridge: Dynamics and magmatism of a mantle plume and its influence on the Tonga-Kermadec subduction system.* Technical report. Universitat Kiel, page 276.

Stoffers, P., T. J. Worthington, U. Schwarz-Schampera, M. D. Hannington, G. J. Massoth, R. Hekinian, M. Schmidt, L. J. Lundsten, L. J. Evans, R. Vaiomo'unga, and T. Kerby (2006). "Submarine volcanoes and high-temperature hydrothermal venting on the Tonga arc, southwest Pacific". *Geology* 34(6), page 453. DOI: 10.1130/g22227.1.

Symons, G. J., J. W. Judd, S. R. Strachey, W. J. L. Wharton, F. J. Evans, F. A. R. Russell, D. Archibald, and G. M. Whipple (1888). *The eruption of Krakatoa, and subsequent phenomena.* London: Trübner & Co.

Walker, S. L., C. E. J. de Ronde, M. Williams, K. Zwolak, and B. Simpson (2022). "Ongoing Activity Within the Submarine Caldera of Hunga Tonga - Hunga Ha'apai Volcano, Tonga, Six Months After the Eruption of January 15, 2022". *AGU Fall Meeting Abstracts*. Volume 2022, V16A-02, V16A–02.

Wang, X., W. Randel, Y. Zhu, S. Tilmes, J. Starr, W. Yu, R. Garcia, O. B. Toon, M. Park, D. Kinnison, J. Zhang, A. Bourassa, L. Rieger, T. Warnock, and J. Li (2023). "Stratospheric Climate Anomalies and Ozone Loss Caused by the Hunga Tonga-Hunga Ha'apai Volcanic Eruption". *Journal of Geophysical Research: Atmospheres* 128(22). DOI: 10.1029/2023jd039480.

Wessel, P. and W. H. F. Smith (1998). "New, improved version of generic mapping tools released". *Eos, Transactions American Geophysical Union* 79(47), pages 579–579. DOI: 10.1029/98eo00426.

Whiteside, A., C. Dupouy, A. Singh, P. Bani, J. Tan, and R. Frouin (2023). "Impact of ashes from the 2022 Tonga volcanic eruption on satellite ocean color signatures". *Frontiers in Marine Science* 9. DOI: 10.3389/fmars.2022.1028022.

Witter, J. B. and S. Self (2006). "The Kuwae (Vanuatu) eruption of AD 1452: potential magnitude and volatile release". *Bulletin of Volcanology* 69(3), pages 301–318. DOI: 10.1007/s00445-006-0075-4.

Wölfl, A.-C., H. Snaith, S. Amirebrahimi, C. W. Devey, B. Dorschel, V. Ferrini, V. A. I. Huvenne, M. Jakobsson, J. Jencks, G. Johnston, G. Lamarche, L. Mayer, D. Millar, T. H. Pedersen, K. Picard, A. Reitz, T. Schmitt, M. Visbeck, P. Weatherall, and R. Wigley (2019). "Seafloor Mapping – The Challenge of a Truly Global Ocean Bathymetry". *Frontiers in Marine Science* 6. DOI: 10.3389/fmars.2019.00283.

Wright, I. and J. Gamble (1999). "Southern Kermadec submarine caldera arc volcanoes (SW Pacific): caldera formation by effusive and pyroclastic eruption". *Marine Geology* 161(2–4), pages 207–227. DOI: 10.1016/s0025-3227(99)00040-7.

Wright, I., T. Worthington, and J. Gamble (2006). "New multibeam mapping and geochemistry of the 30°–35° S sector, and overview, of southern Kermadec arc volcanism". *Journal of Volcanology and Geothermal Research* 149(3–4), pages 263–296. DOI: 10.1016/j.jvolgeores.2005.03.021.

Yuen, D. A., M. A. Scruggs, F. J. Spera, Y. Zheng, H. Hu, S. R. McNutt, G. Thompson, K. Mandli, B. R. Keller, S. S. Wei, Z. Peng, Z. Zhou, F. Mulargia, and Y. Tanioka (2022). "Under the surface: Pressure-induced planetary-scale waves, volcanic lightning, and gaseous clouds caused by the submarine eruption of Hunga Tonga-Hunga Ha'apai volcano". *Earthquake Research Advances* 2(3), page 100134. DOI: 10.1016/j.eqrea.2022.100134.